Melting transition in a quasi-two-dimensional colloid suspension: Influence of the colloid-colloid interaction

Pallop Karnchanaphanurach, Binhua Lin, and Stuart A. Rice
James Franck Institute and The Department of Chemistry, The University of Chicago, Chicago, Illinois 60637
(Received 22 June 1999)

We report the results of a study, using digital video microscopy, of the melting transition in a quasi-two-dimensional suspension of uncharged silica spheres. This system was chosen to further test the dependence of the two-dimensional melting transition on the functional form of the colloid-colloid interaction. Our experimental data show that the solid phase undergoes a first order transition directly to the liquid phase. The system studied yields no evidence of the existence of a hexatic phase interpolating between the solid and liquid phases in the melting process.

PACS number(s): 82.70.Dd

I. INTRODUCTION

The melting transition in a two-dimensional system has been the subject of intense investigations for more than two decades. This transition is of great theoretical interest because the type of order that distinguishes the solid phase from the liquid phase is qualitatively different from that in three dimensions. In the three-dimensional case the density-density correlation function of the ordered solid phase decays, with increasing particle separation, to a nonzero constant value in the limit of infinite separation. This is the characteristic feature of long-range positional order. In the two-dimensional case the density-density correlation function of the solid phase decays to zero algebraically in the limit of infinite particle separation, which is the characteristic feature of quasi-long-range order. There is, in a two-dimensional system, a special kind of long-range order called bond orientation order. According to the Kosterlitz-Thouless-Halperin-Nelson-Young (KTHNY) theory [1–5], two-dimensional solids melt via successive dislocation unbinding and disclination unbinding transitions; for most systems it is expected that these will be sequential continuous phase transitions. The first transition is from the solid with quasi-long-range positional order and long-range bond orientation order to a phase with short-range positional order and quasi-long-range bond orientation order, the so called hexatic phase. The second transition transforms a hexatic phase to a liquid phase in which both the positional and bond orientation orders are short ranged. However, other pathways for two-dimensional melting can occur. For example, it is possible for the dislocation unbinding transition to be preempted by grain-boundary-induced melting, as suggested by Chui [6].

It should be noted that the KTHNY theory of melting in two-dimensional systems is not based on any particular choice of functional form for the intermolecular potential energy. Rather, the theory is based on a free energy functional that represents the two-dimensional solid as a continuous elastic medium. This free energy functional also includes the contributions from the two classes of point topological defects with smallest excitation energy. It is then reasonable to expect that the theoretical description of melting should be valid for any two-dimensional system that can be characterized as an elastic medium. Then the character of the melting transition should not depend on the form of the particle-particle interaction except through its influence on the elastic constants of the system. However, the KTHNY theory is not a thermodynamically consistent theory of melting. Rather, it is an analysis of the limit of stability of a two-dimensional solid (as is also the Chui analysis), since it neglects the existence of the liquid phase and thereby does not impose an equality of the chemical potentials of the solid and liquid phases as the criterion for melting. Consequently, it remains possible that the character of the melting transition in two-dimensional systems can be sensitive to the form of the particle-particle potential. An indication of the existence of this sensitivity is provided in the work of Bladon and Frenkel [7]. These investigators reported the results of simulations of a two-dimensional assembly of disks which interact via a pair additive potential consisting of a hard core repulsion and a very narrow square well attraction (or a very narrow step repulsion). When the width of the attractive well is less than 8% of the hard disk diameter, the system supports two ordered solid phases with the same packing symmetry but different densities. The locus of the isostructural solid-solid transition line ends at a critical point, near which density fluctuations render the solid unstable with respect to dislocation unbinding, and the system supports a hexatic phase. When the square well width is not close to the limiting value for which the lower density solid phase becomes unstable, the region of stability of the hexatic phase lies between those of the two solid phases. For the case when the square well width is close to the limiting value for which the lower density solid phase becomes unstable, the hexatic region can extend to the melting line. Then the sequence of transitions becomes solid-to-hexatic-to-liquid rather than solid-to-hexatic-to-solid. The liquid-to-hexatic transition is predicted to be first order, while the hexatic-to-solid transition may be either first or second order. We note that the results of the Bladon-Frenkel analysis are very sensitive to the width of the well, and that the region of stability of the hexatic phase shrinks drastically as the width of the well decreases. In the limit that the well width becomes zero the melting transition is first order; it is also predicted to be first order when the well width is of order 1% of the hard disk diameter.

The prediction of the Bladon-Frenkel analysis of a first order melting transition in a two-dimensional system of hard disks is just one of an inconclusive set of predictions derived

from simulation studies of that system. Just two examples, drawn from recent simulation studies, suffice to summarize the current status of this set of predictions. In agreement with the Bladon-Frenkel result, Weber, Marx, and Binder [8] reported that the melting of a two-dimensional system of hard disks is a first order transition. However, the most recent study of the two-dimensional hard disk system, by Jaster [9], concludes that melting can be either a weak first order transition with an interface width that is larger than the largest simulation sample studied, or a continuous transition.

Many experimental investigations of quasi-two-dimensional systems have been carried out to test the continuity of the solid-to-hexatic and hexatic-to-liquid phase transitions and to examine the character of the hexatic phase. Recent advances in technology have allowed the use of monodisperse colloid suspensions for these studies. By tailoring the length of the stabilizing polymeric brush attached to a colloid particle, or by choosing additive polymers of different radii of gyration, the particle-particle and particle-wall interactions of colloid systems can be adjusted to vary from short ranged to long ranged. Taking advantage of the size of the colloid particle, digital video microscopy can be used to measure the positional order and the bond-orientation order in the colloid suspension. The data obtained via digital video microscopy also include the densities and structures of various defects, and their dynamical behavior in real space. Also, quasi-two-dimensional colloid suspensions can be very large on the scale of the positional and bond-orientation correlation lengths, thereby eliminating problems associated with boundary conditions.

The extant literature contains several examples of the use of colloid suspensions to study melting in quasi-two-dimensional systems [10–14]. The results obtained by Murray and Van Winkle from studies of suspensions of charge-stabilized polystyrene spheres in a wedge shaped cell [11] are consistent with the behavior predicted by KTHNY theory. On the other hand, the results obtained by Marcus and Rice [14] from studies of sterically stabilized uncharged polymethylmethacrylate (PMMA) particles confined in a uniform thickness cell reveal the existence of first order solid-to-hexatic and hexatic-to-liquid transitions. The form of the interaction between sterically stabilized colloid particles is very different from that between charged colloid particles. Marcus and Rice inferred, from their experimental data, that the interaction between the sterically stabilized PMMA particles they studied had a generic resemblance to the form of the potential used in the Bladon and Frenkel simulations. Figure 1(a) displays the form of the particle-particle interaction inferred; it has a hard core of diameter σ, a soft repulsive interaction in the range $\sigma<R<1.04\sigma$, and a narrow weak attractive well centered at about 1.05σ (width about 0.01σ and depth about k_BT). Zangi and Rice [15] reported the results of molecular dynamics simulations of a quasi-two-dimensional system of particles using the colloid-colloid interaction displayed in Fig. 1(a). The quasi-two-dimensional character of the system was established by using an external potential to restrict the out-of-plane motion of a colloid particle to a range commensurate with the thickness of the cell used in the Marcus-Rice experiments. The results obtained reproduced all the major features of the Marcus-Rice experiments, in particular the existence of first order

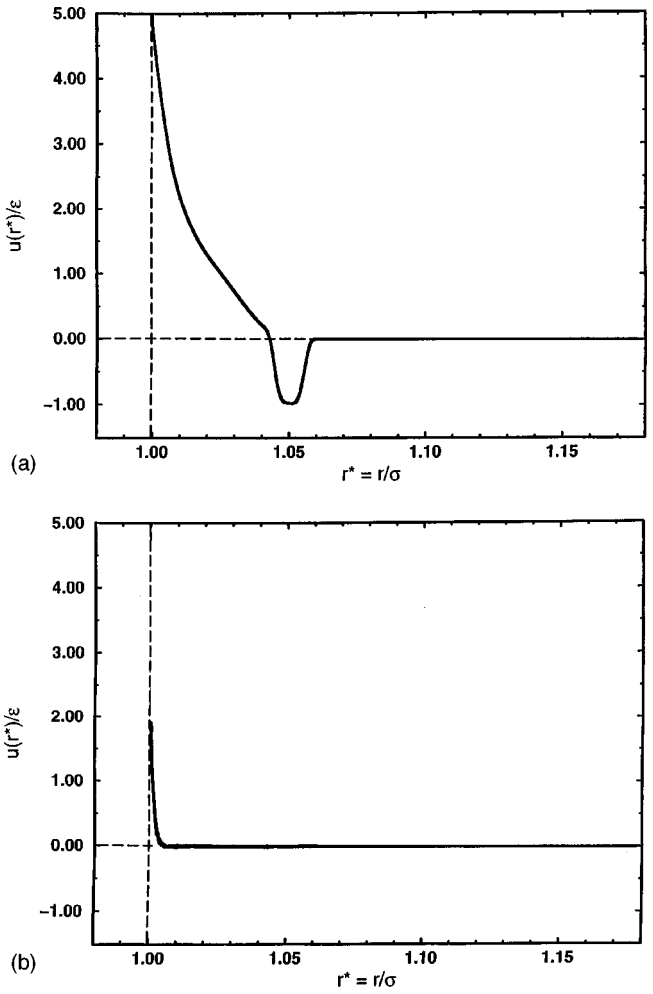

FIG. 1. (a) The Marcus-Rice potential for sterically stabilized PMMA particles. (b) The potential inferred for sterically stabilized silica particles.

transitions between the liquid and hexatic phases and between the hexatic and solid phases. Zangi and Rice also found that the simulated system exhibits an isostructural solid-to-solid transition and a buckling transition, and that the dislocation pair, free dislocation, and disclination concentrations do not agree with the predictions of the KTHNY theory.

In this paper we present the results of studies of suspensions of uncharged silica colloid particles confined in a quasi-two-dimensional uniform thickness cell. This system was chosen to further test the influence of the range of the colloid-colloid interaction on the melting transition in the quasi-two-dimensional system by comparison of the results obtained with the results reported by Marcus and Rice. The PMMA particles used by Marcus and Rice were about 1 μm in diameter, and they were covered with a polymer brush about 30 nm thick. The silica particles used in the studies reported in this paper are 1.58 μm in diameter, and they are covered with a 12-carbon-surfactant ($\sim$1.7 nm). We expect, then, that the silica particle-particle interaction will have a hard core of diameter σ and a soft repulsive interaction in the range $\sigma<R<1.002\sigma$ [see Fig. 1(b)]. For a potential that consists of a hard core and a very short-ranged square well repulsion (or attraction), overall like the potential shown in

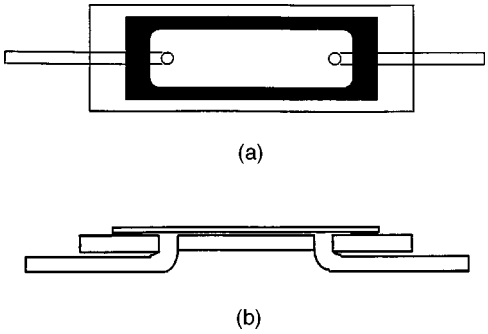

FIG. 2. (a) Top view. (b) Side view. One glass microscope slide, one glass coverslip, and two bent pieces of glass tubing are glued together with epoxy. The shaded region represents the space between the cover slip and the slide that is filled with epoxy. The sample is loaded into the cell through the tubing that is part of a closed manifold system which may be partially evacuated and thereby adjusts the distance between the cell walls.

Fig. 1(b), Bladon and Frenkel found only a first order melting transition in the two-dimensional system. Zangi and Rice [13] reported the results of molecular dynamics simulations of a quasi-two-dimensional system of particles using a modified Marcus-Rice colloid-colloid interaction that lacks the attractive well shown in Fig. 1(a). This potential is everywhere repulsive, albeit in the range $\sigma<R<1.04\sigma$ it is soft. Zangi and Rice found that this colloid assembly also undergoes first order solid-to-hexatic and hexatic-to-liquid transitions, and a solid-to-solid buckling transition. The sensitivity of the character of the two-dimensional melting transition to the functional form of the colloid-colloid interaction is reminiscent of the difference between the findings of Bagchi, Anderson, and Swope [16] and Weber, Marx, and Binder [8] for the two-dimensional melting transition with, respectively, R^{-12} and hard core interactions. In the former case the authors of Ref. [16] reported that melting is continuous with a very small region of stability for the hexatic phase; in the latter case, as already noted, the authors of Ref. [8] reported that the melting is a first order transition.

In this paper we report experimental evidence for a difference between the character of two-dimensional melting in colloid assemblies in which the colloid-colloid interaction is, in one case, of the Marcus-Rice type [Fig. 1(a)] and, in the other case, softly repulsive in the range $\sigma<R<1.002\sigma$ [Fig. 1(b)]. The experimental data described below show that the ordered solid phase of quasi-two-dimensional sterically stabilized silica spheres undergoes a first order transition directly to the liquid phase, with no evidence of an intermediate hexatic phase in the melting process.

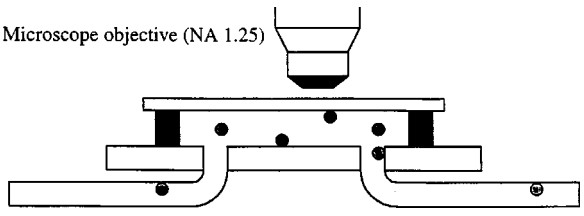

FIG. 3. Side view of a cell with two reference particles (colored black); objects are exaggerated for clarity.

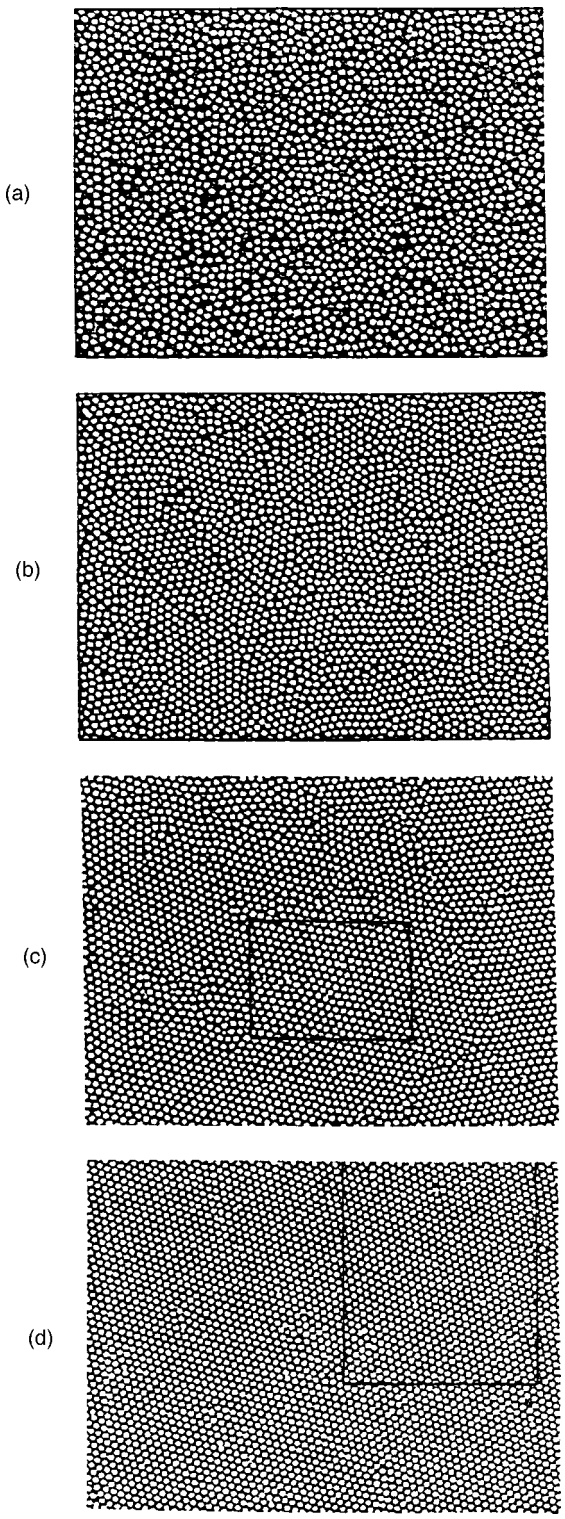

FIG. 4. Sample particle configurations with frame size 640×480 pixel^2 ($114\times85\ \mu$m^2) (a) Liquid phase. (b) Coexistence between liquid and solid phases. (c) Solid near melting. (d) Compressed solid. The marked subblocks are the regions used to calculate the two-dimensional structure functions.

II. EXPERIMENTAL METHOD

We have studied the properties of quasi-two-dimensional suspensions of sterically stabilized silica spheres in water (obtained from Duke Scientific). The uniform spheres had a diameter $\sigma=1.58\pm0.06\ \mu$m, and the surface of each sphere

TABLE I. Characteristic features of the experimental samples. The density is in units of particle number per frame area normalized by the square of the particle diameter ($N\sigma^2/A$).

ρ^*	Diffraction pattern	Thermodynamic state
0.558	isotropic	liquid
0.619	isotropic	liquid
0.648	superposition of isotropic intensity distribution and Lorentzian line shape	liquid-solid coexistence
0.684	superposition of isotropic intensity distribution and Lorentzian line shape	liquid-solid coexistence
0.704	sixfold modulation Lorentzian line shape	solid
0.708	sixfold modulation Lorentzian line shape	solid
0.725	sixfold modulation Lorentzian line shape	solid
0.761	sixfold modulation Lorentzian line shape	solid
0.767	sixfold modulation Lorentzian line shape	solid
0.775	sixfold modulation Lorentzian line shape	solid
0.799	sixfold modulation Lorentzian line shape	solid
0.832	sixfold modulation Lorentzian line shape	solid
0.847	sixfold modulation Lorentzian line shape	solid
0.856	sixfold modulation Lorentzian line shape	solid
0.876	sixfold modulation Lorentzian line shape	solid
0.915	sixfold modulation Lorentzian line shape	solid
0.987	sixfold modulation Lorentzian line shape	solid
1.05	sixfold modulation Lorentzian line shape	solid

was covered with 12-carbon surfactant. The cells varied in thickness between 1.62 and 1.80 μm, i.e., between 1.025σ and 1.137σ. The sample cells were constructed from glass microscope slides, 0.18-mm-thick microscope cover slips, and glass tubing (4-mm outer diameter). Two 0.33-cm holes separated by 1.90 cm were drilled through the microscope slides. All glass components were coated with the Glassclad® 6*C* and then oven baked at 110 °C for about 15 min to cure the coating material. A nonleaching epoxy (Epo-tek 302 3M, Epoxy Technologies, Inc.) was used to glue the tubing to the slides. The cover slips were glued to the opposite side of the slide surface using an epoxy (Norland Optical Adhesive, Norland Products, Inc.) that cures when exposed to the UV light source. A schematic diagram of a sample cell is displayed in Fig. 2.

The finished cells were loaded with sample in the following manner. First, the cell was flooded with purified, deionized water. Then the colloid suspension was introduced, following which the glass tubing was connected to a manifold constructed from Tygon tubing and a Nalgene hand vacuum pump (Fisher Scientific). The latter was used to adjust the sample cell thickness by reducing the hydrostatic pressure exerted by the suspension in the cell. Each sample cell was examined under a microscope to determine if it contained a quasi-two-dimensional suspension. Two criteria were used to make that judgment, namely, that the particle centers lay in a plane and that cut-of-plane motion of the particles was suppressed.

The properties of the suspensions in the sample cells were studied using Digital Video Microscopy (DVM). The DVM apparatus consisted of an Olympus BH2 metallurgical microscope with a 100× oil immersion objective that has a numerical aperture 1.25, and a Hitachi charge-coupled-device (CCD) video camera to capture images of the suspension. The frame grabbing frequency of the CCD was 30 Hz, while its shutter speed was $\frac{1}{100}$ s. The analog camera output was sent to the video port of a computer-controlled Sanyo GVR-S955 VCR which also passed the image signals to a Power

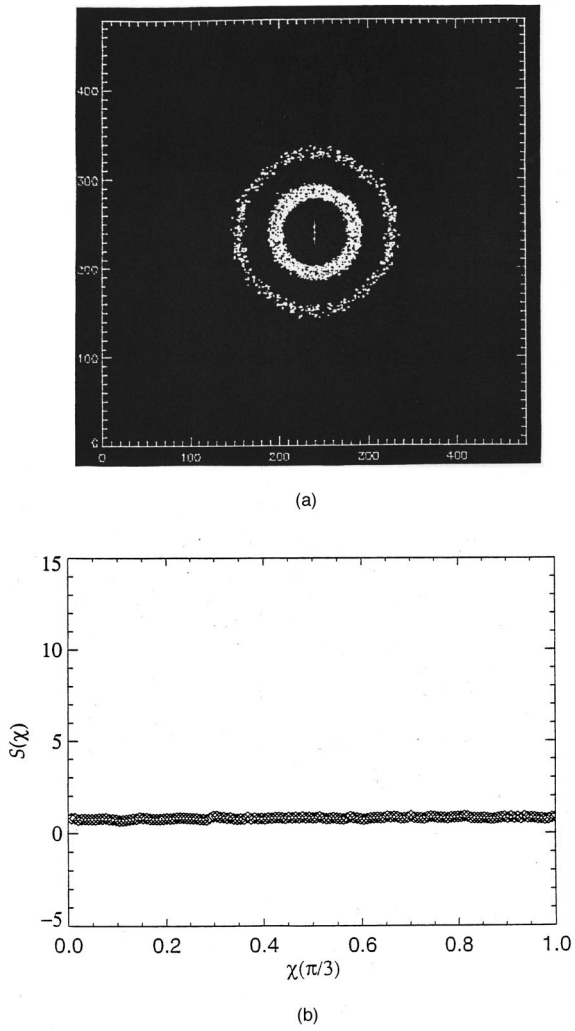

FIG. 5. (a) Diffraction pattern of the sample with $\rho^* = 0.558$. (b) Angular dependence of the line shape of the diffraction pattern for $\rho^* = 0.558$.

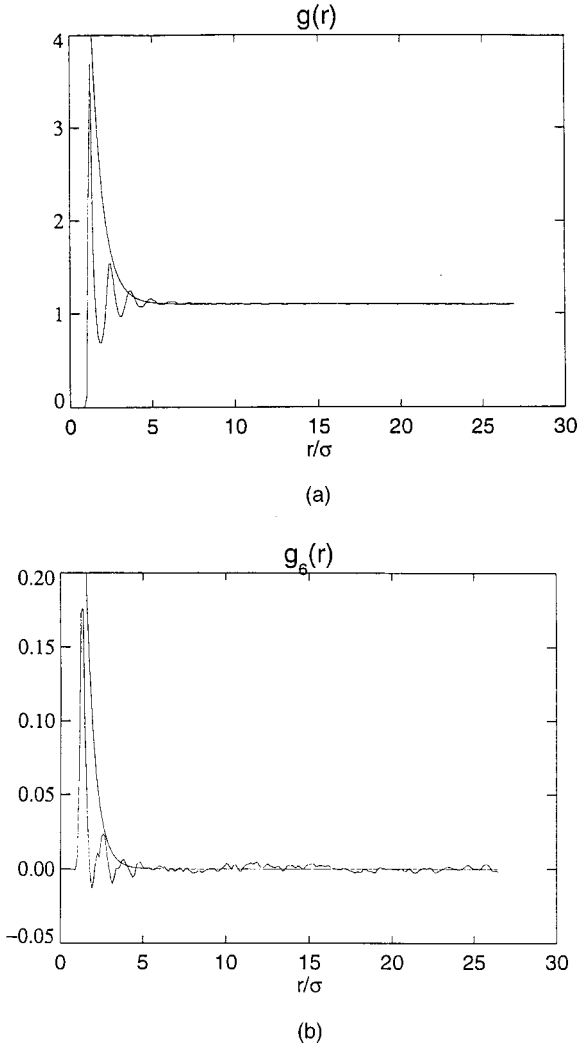

FIG. 6. (a) Pair correlation function of the sample with $\rho^* = 0.558$. The envelope of $g(r)$ decays exponentially ($\sim e^{(-r/0.7\sigma)}$). (b) Bond orientation correlation function of the sample with $\rho^* = 0.558$. The envelope of $g_6(r)$ decays exponentially ($\sim e^{(-r/0.55\sigma)}$).

Macintosh G3 computer where most of the data analysis was carried out. The Scion Image 1.60*c* software package was used to directly frame grab 640×480 square-pixel images on the computer and another Sanyo VCR was used to record the images on an S-VHS video cassette tape for backup purposes. All image processing procedures and data analyses were implemented using IDL (Research Systems, Inc.), a programming language designed for visual data analysis. The pixel size was calibrated by imaging a gold grid of known scale. The pixels were square as was verified by calibration in the *x* and *y* directions. The calibrated pixel size was determined to be 0.178 μm/pixel.

In all of our experiments the sample cell thickness was adjusted to be between 1.03 and 1.14 particle diameters ($\sim$1.62 to 1.80 μm). When the DVM measurements of a sample suspension were complete, the difference between internal pressure in the cell and atmospheric pressure was reduced to zero, and the cell was rinsed with pure water to greatly dilute the suspension. The internal-external pressure difference was then returned to the same value as when the DVM measurements were made. We assumed that the cell thickness was in one-to-one correspondence with the internal-external pressure difference. In each cell there were a few spheres fixed to each wall (see Fig. 3), which we used as reference markers. Specifically, we measured the difference between the positions of the focal planes of the centers of the fixed particles using the microscope fine focus control. A single-axis motion controller (Newport Corp.) connected directly to the microscope fine focus control was used to read it. The accuracy of this technique is ± 0.15 μm.

The images of the systems we have studied provide direct evidence that the centers of the colloid particles are closely confined to a plane with very little out-of-plane motion. The properties of these quasi-two-dimensional colloid suspensions were studied over the two-dimensional density range $0.558 \leqslant \rho^* = \rho\sigma^2 \leqslant 1.05$. The observable in a DVM experiment is a complete set of two-dimensional particle trajectories, which can be used to define the time-dependent density

$$\rho(\mathbf{r},t) = \sum_{i=1}^{N} \delta(\mathbf{r} - \mathbf{r}_i(t)). \tag{2.1}$$

The process of transforming the information contained in a sequence of digitized images into the time-dependent density

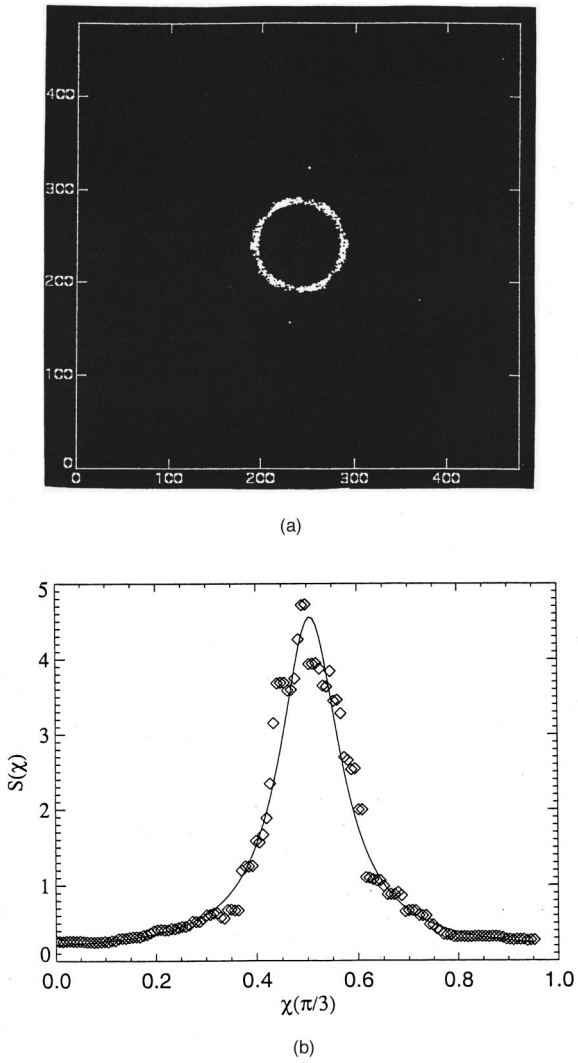

FIG. 7. (a) Diffraction pattern of the sample with $\rho^* = 0.684$. (b) Angular dependence of the distribution of intensity in the diffraction pattern when $\rho^* = 0.684$. The solid line is the fit to the superposition of an isotropic background intensity (for the liquid phase) and a Lorentzian function (for the solid phase). The Lorentzian function has the form $0.12 + 0.023[(\chi - 0.51\ \text{rad})^2 + (0.073\ \text{rad})^2]^{-1}$.

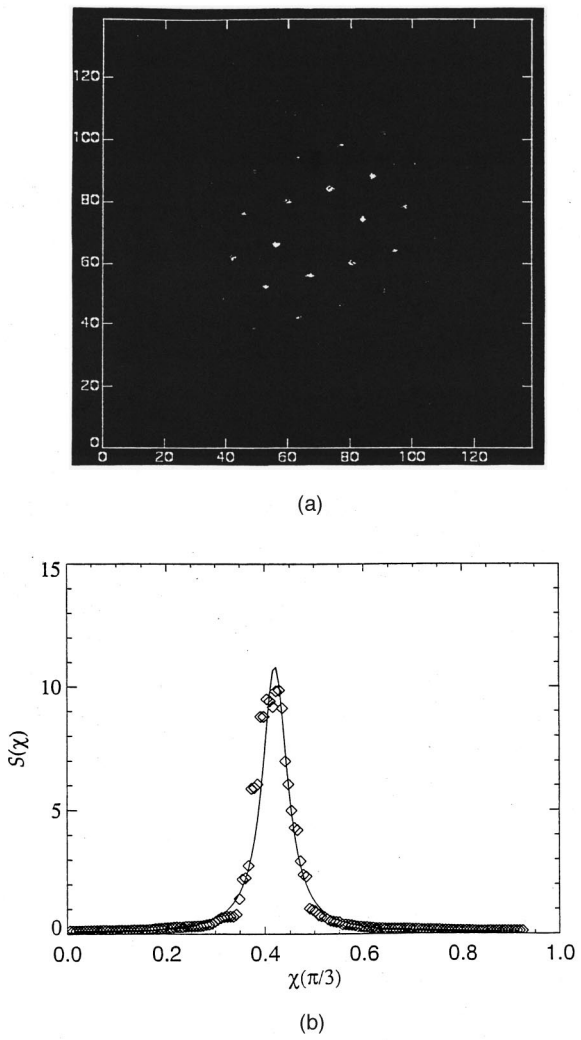

FIG. 8. (a) Diffraction pattern of the sample with $\rho^* = 0.704$. (b) Angular dependence of the line shape of a peak in the diffraction pattern when $\rho^* = 0.704$. The solid line is the fit to the Lorentzian function, $0.0097[(\chi - 0.42\ \text{rad})^2 + (0.0299\ \text{rad})^2]^{-1}$.

profile described by the above equation is discussed elsewhere [17,18]. The trajectory data obtained were used to calculate correlation functions and other static quantities of interest.

III. RESULTS

When the packing density was high, almost every suspension we studied exhibited a number of line boundaries that divide it into homogeneous patches. The frequent appearance of these boundaries is an expected consequence of our use of very thin cells ($1.025\sigma < H < 1.137\sigma$), where H is the cell thickness. In these thin cells the time required to anneal out all defects is very great. If it is assumed that the true equilibrium state is a single macroscopic ordered domain, we must conclude that our samples were locked into a very near equilibrium state. Just as in the case of a polycrystalline bulk metal, we expect the structure of a homogeneous region to be negligibly different from that of the (infinite) system at equilibrium.

To make sensible identifications of the several phases, we limited the structure factor analysis to homogeneous subregions of a regular 640×480 square-pixel image. The outlined areas in Figs. 4(c) and 4(d) show such subregions. There is no reason to believe that the resulting structure function, which is itself a Fourier transform in space of the density-density correlation function, does not identify the true character of the phase examined.

Table I displays the density, the nature of the powder diffraction pattern, and the thermodynamic state of each sample under investigation. Figure 4 shows the sample configurations at four densities: $\rho^* = 0.558$, 0.684, 0.708, and 0.847. Proceeding from the lowest density to the highest density, these figures show (a) a liquid phase, (b) a state with coexistence between liquid and solid phases, (c) a solid close to melting, and (d) a dense solid. We will discuss the properties of these phases below.

We computed the static structure function from

$$S(\mathbf{k})=\frac{1}{N}\sum_i\sum_j\langle\exp[i\mathbf{k}\cdot(\mathbf{r}_i-\mathbf{r}_j)]\rangle. \tag{3.1}$$

Figure 5(a) shows the two-dimensional structure function corresponding to the entire sample with density $\rho^*=0.558$. Figure 5(b) shows the transverse angular dependence of the diffraction peak. Since the diffraction peak has no transverse angular dependence, this sample is an isotropic liquid. This inference is supported by the observation that the pair correlation function, and the bond orientation correlation function are short ranged. Figure 6(a) displays the pair correlation function computed from

$$g(r)=\frac{1}{\rho^2}\left\langle\sum_i\sum_{j\neq i}\delta(\mathbf{r}_i)\,\delta(\mathbf{r}_j-\mathbf{r})\right\rangle. \tag{3.2}$$

The global bond-orientation correlation function displayed in Fig. 6(b) was calculated from

$$g_6(r)=\frac{\langle\psi_6^*(0)\,\psi_6(r)\rangle}{\langle\delta(r_i)\,\delta(r_j-r)\rangle}\propto r^{-\eta_6(T)}, \tag{3.3}$$

with $0\leqslant\eta_6\leqslant\frac{1}{4}$, and

$$\psi_6(r_i)=\left\langle\frac{1}{N}\sum_j\exp[6i\,\theta(r_{ij})]\right\rangle. \tag{3.4}$$

In Eq. (3.3), $\psi_6(r_i)$ is the local bond orientation order parameter, where the index j counts the nearest neighbors to particle i, $\theta(r_{ij})$ is the angle between the line connecting particle i and j and an arbitrary fixed reference axis, and N is the number of i-j bonds. In Eq. (3.4), the index i runs over all particles, and j counts the nearest neighbors to particle i. We note that the correlation functions displayed in Figs. 6(a) and 6(b), which exhibit exponentially decaying envelopes, are both short ranged.

Coexistence between liquid and solid phases is strongly suggested by the diffraction pattern from the system with density $\rho^*=0.684$, shown in Fig. 7(a). This diffraction pattern is a superposition of that for an isotropic liquid and that for a hexagonal solid. As shown in Fig. 7(b), the transverse angular dependence of the diffraction peak can be described well with the superposed line shapes for diffraction from coexisting liquid (the nonzero isotropic scattering) and a solid phase. Similar results are obtained when the density is $\rho^*=0.648$.

When the density is $\rho^*=0.704$, the system is in an ordered hexagonal phase. The diffraction pattern shown in Fig. 8(a) has a clearly developed sixfold angular symmetry. The transverse angular dependence of a diffraction peak is very well described by the Lorentzian function

$$S(\theta_0)=[(\theta_0-\chi)^2+\kappa^2]^{-1}, \tag{3.5}$$

where θ_0 is the angular position of the first peak in the diffraction pattern, χ is the in-plane angle, and κ is the width of the peak. It is not known if $\rho^*=0.704$ is the low-density limit of stability of the ordered solid because the spacing in density of our samples is rather coarse. For the same reason we cannot identify the high-density limit of the stability of the liquid phase. It appears, from the data available, that the liquid-solid coexistence region extends from somewhat below $\rho^*=0.648$ to somewhat below $\rho^*=0.704$. If these estimates are correct, our system exhibits a strong first order freezing-melting transition.

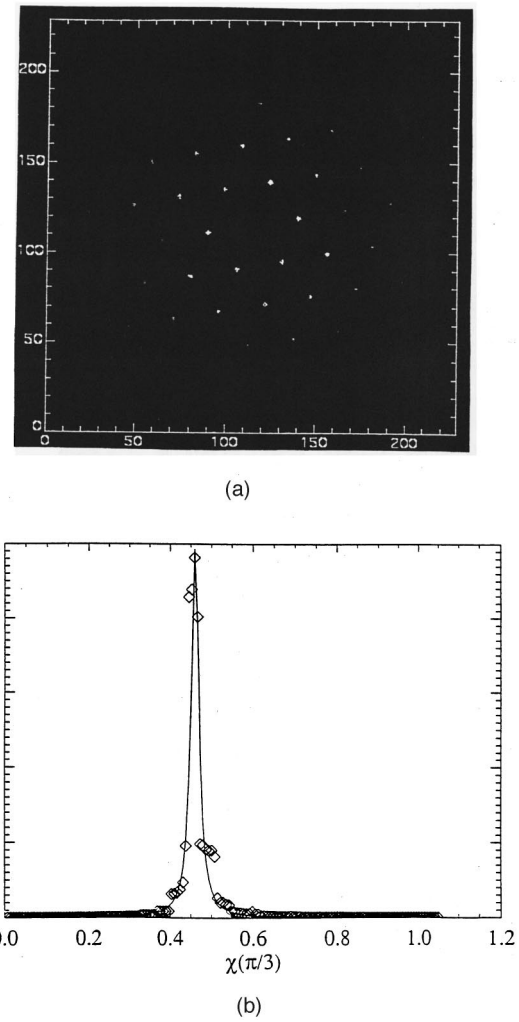

FIG. 9. (a) Diffraction pattern of the sample with $\rho^*=0.847$. (b) Angular dependence of the line shape of a peak in the diffraction pattern when $\rho^*=0.847$. The solid line is the fit to the Lorentzian function, $0.00635[(\chi-0.46\,\text{rad})^2+(0.0113\,\text{rad})^2]^{-1}$.

It should be mentioned that none of the transverse angular shapes of diffraction peaks calculated from our experimental data can be fitted to a square-root Lorentzian line-shape function,

$$S(\theta_0)=[(\theta_0-\chi)^2+\kappa^2]^{-1/2}. \tag{3.6}$$

Since the square-root Lorentzian line shape function has been established as a signature of hexatic order [19,20], none of our data indicates the existence of a hexatic phase.

When $\rho^*=0.847$, the quasi-two-dimensional colloid suspension is in a compressed solid phase. The diffraction pattern at this density [Fig. 9(a)] displays very sharp peaks and sixfold symmetry. As shown in Fig. 9(b), the transverse angular dependence of a peak in this diffraction pattern is very well described by a Lorentzian function. The conclusion that this sample is an ordered solid is supported by the observa-

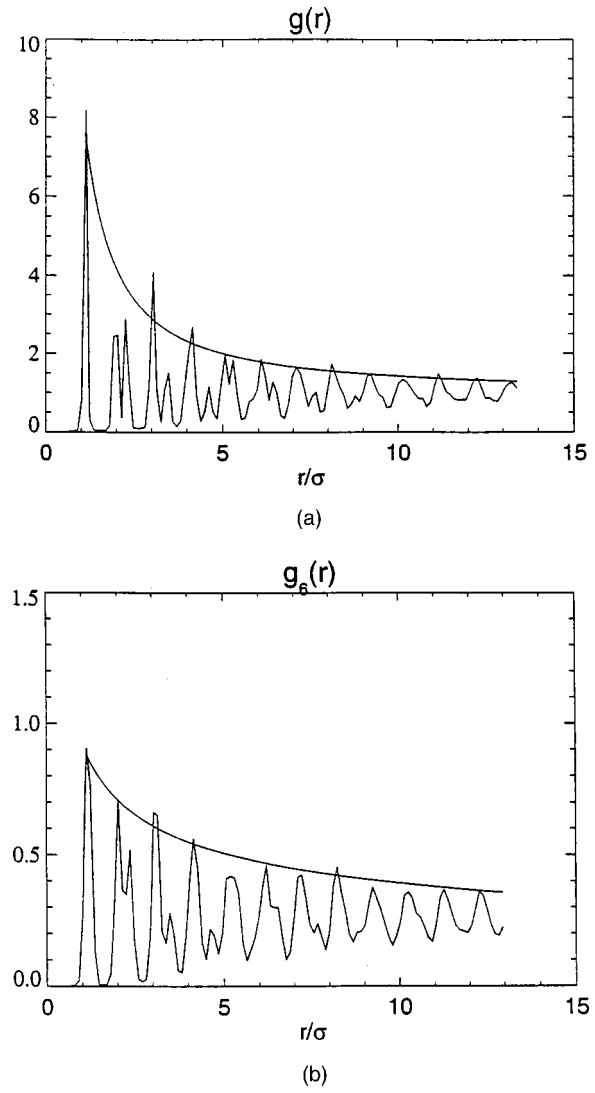

FIG. 10. (a) Translational correlation function of the sample with $\rho^*=0.847$. The envelope of $g(r)$ decays algebraically $[\sim(r/\sigma)^{-1/0.8}]$. (b) Bond orientation correlation function when $\rho^*=0.847$. The envelope of $g_6(r)$ decays algebraically $[\sim(r/\sigma)^{-1/2.7}]$.

tions that the positional correlation function appears to exhibit quasi-long-ranged, and that the bond order correlation function appears to be long ranged [see Figs. 10(a) and 10(b)].

The density dependence of the distribution of local bond orientation order parameters for different overall sample densities is shown in Figs. 11(a)–11(e). The distribution of the local density for different overall sample densities is shown in Figs. 11(f)–11(j). As expected, the average values of the local bond orientation order parameter and the local density increase as the sample density increases.

We define the local density by

$$\rho(r_i)=1/A_i\,, \tag{3.7}$$

with A_i the area of the Voronoi polygon assigned to particle i. The overall sample densities on passage from Figs. 11(a)–11(e) and from Figs. 11(f)–11(j) are 0.558, 0.619, 0.684, 0.847, and 0.915, respectively. In the pure liquid [Figs. 11(a) and 11(b)] and pure solid phases [Figs. 11(d) and 11(e)], the local bond orientation order parameter and the local-density distributions are unimodal. When the overall sample density is 0.684 [Fig. 11(c)], the local bond orientation order parameter distribution is bimodal, indicating coexistence between two phases. As previously discussed, those are necessarily the liquid and solid phases. Note that one peak of this bimodal distribution is located at the same place as in the ordered solid, and the other is clearly at the same place as in the liquid phase. However, at this overall sample density the local density distribution appears to be unimodal on the mesh of density displayed [Fig. 11(h)]. This result appears to be inconsistent with the estimated density change across the transition ($\Delta\rho^*\approx 0.056$). However, the mesh of local density values is coarse enough to obscure the existence of slightly separated overlapping distributions of the local density.

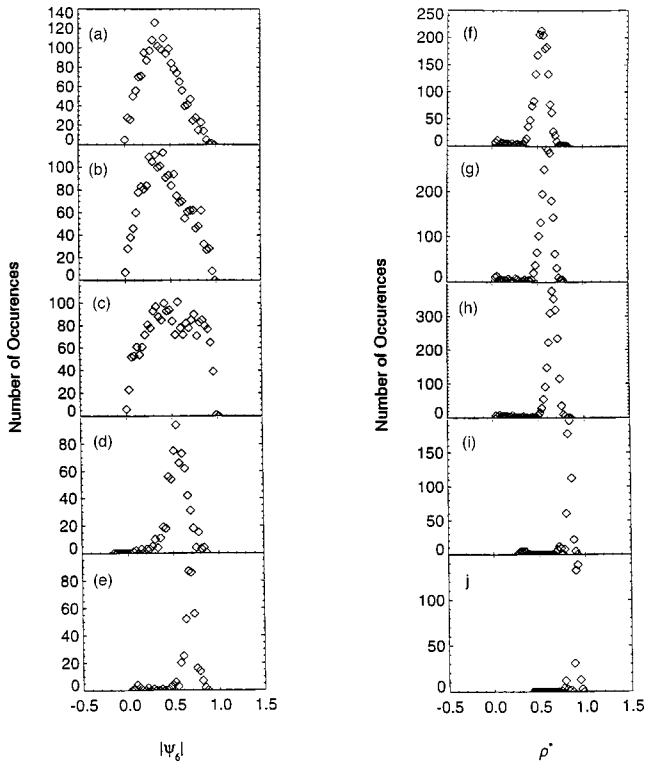

FIG. 11. The distributions of local bond orientation order parameters at the overall sample densities (a) 0.558, (b) 0.619, (c) 0.684, (d) 0.847, and (e) 0.915, and the distributions of the local density for the overall sample densities (f) 0.558, (g) 0.619, (h) 0.684, (i) 0.847, and (j) 0.915.

IV. SUMMARY

The principal finding of the experiments reported in this paper is that a quasi-two-dimensional suspension of sterically stabilized uncharged silica spheres undergoes a first order melting transition. Our data provide no evidence for the existence of a hexatic phase interpolated between the solid and liquid phases of this system.

Our argument for the conclusion stated above is based on an analysis of the calculated diffraction patterns for samples of the quasi-two-dimensional colloid suspension with different densities, and the character of the density dependence of

the local bond orientation order parameter distribution function. In particular, the calculated diffraction pattern for $\rho^* = 0.648$ (not shown) and for $\rho^* = 0.684$ strongly suggests the coexistence of isotropic and sixfold modulated scattering, and the distribution of local bond-orientation order parameters is bimodal. Both of these results are consistent with the coexistence of solid and liquid phases, which is the unique signature of a first order phase transition.

The absence of hexatic phase between the solid and liquid phases is consistent with what we believe to be the form of the colloid-colloid interaction in the system studied. The uncharged silica spheres used in this experiment were coated with a short chain surfactant whose length, ~1.7 nm, is only ~0.1% of the particle diameter. In this sense they are very nearly hard spheres. The results we have obtained differ from those found in the simulations recently reported by Jaster [9] in two respects. Jaster reported that melting in a two-dimensional hard disk system is consistent with the KTHNY theory or is a weak first order transition with a liquid-solid interface width that is larger than the homogeneous domains used to analyze the system properties. We find that our quasi-two-dimensional nearly hard sphere system has a strong first order melting transition with a well defined coexistence region. Our results are qualitatively consistent with the results of Bladon and Frenkel's simulations of the melting of a two-dimensional assembly of particles with a hard disk plus very short ranged attraction (or repulsion) interaction. As noted earlier, these simulations show that the melting transition is first order when the width of the attractive well (or the repulsive shoulder) is less than 3% of the hard disk diameter. The results of the experiments reported herein, and those reported earlier by Marcus and Rice, suggests that the nature of particle-particle interaction can profoundly influence the character of the melting transition in two-dimensional system.

ACKNOWLEDGMENTS

The research reported in this paper was supported by the Materials Research Science and Engineering Center at the University of Chicago, which is funded by the National Science Foundation through Grant No. MRSEC-543038, and by a grant from the Richter Fund of The University of Chicago (RICHTER-691333). We thank Professor A. H. Marcus, Dr. Ronen Zangi, and Professor John Crocker for their advice and technical assistance.

[1] For a review, see D. R. Nelson, in *Phase Transitions and Critical Phenomena*, edited by C. Domb and J. L. Leibowitz (Academic, London, 1983), Vol. 7.
[2] J. M. Kosterlitz and D. J. Thouless, J. Phys. C **5**, L124 (1972); **6**, 1181 (1973).
[3] B. I. Halperin and D. R. Nelson, Phys. Rev. Lett. **41**, 121 (1978).
[4] D. R. Nelson and B. I. Halperin, Phys. Rev. B **19**, 2457 (1979).
[5] A. P. Young, Phys. Rev. B **19**, 1855 (1979).
[6] S. T. Chui, Phys. Rev. B **28**, 178 (1983).
[7] P. Bladon and D. Frenkel, Phys. Rev. Lett. **74**, 2519 (1995).
[8] H. Weber, D. Marx, and K. Binder, Phys. Rev. B **51**, 14636 (1995).
[9] A. Jaster, Phys. Rev. E **59**, 2594 (1999).
[10] *Bond-Orientational Order in Condensed Matter Systems*, edited by K. J. Strandburg (Springer-Verlag, New York, 1992).
[11] C. A. Murray and D. H. Van Winkle, Phys. Rev. Lett. **58**, 1200 (1988).
[12] C. A. Murray and R. A. Wenk, Phys. Rev. Lett. **62**, 1643 (1989).
[13] C. A. Murray, W. O. Sprenger, and R. A. Wenk, Phys. Rev. B **42**, 688 (1990).
[14] A. H. Marcus and S. A. Rice, Phys. Rev. E **55**, 637 (1997).
[15] R. Zangi and S. A. Rice, Phys. Rev. E **58**, 7529 (1998).
[16] K. Bagchi, H. C. Anderson, and W. Swope, Phys. Rev. E **53**, 3794 (1996).
[17] A. H. Marcus, B. Lin, and S. A. Rice, Phys. Rev. E **53**, 1765 (1996).
[18] J. C. Crocker and D. G. Grier, J. Colloid Interface Sci. **179**, 298 (1996).
[19] S. C. Davey, J. Budai, J. W. Goodby, R. Pindak, and D. E. Moncton, Phys. Rev. Lett. **53**, 2129 (1984).
[20] G. Aeppli and R. Bruinsma, Phys. Rev. Lett. **53**, 2133 (1984).